THE ELASTIC MODULI OF THICK COMPOSITES

E. P. Papadakis, T. Patton,
Y.-M. Tsai, and D. O. Thompson

Center for Nondestructive Evaluation
329 Wilhelm Hall
Iowa State University
Ames, Iowa 50011

INTRODUCTION

Thick composites are in use in critical applications and are proposed for still others. It is important to measure the elastic moduli of thick composites for two reasons: (1) for design data on stiffness, and (2) for prediction of feasible wave paths for ultrasonic waves for NDE. Previously only relatively thin composites of relatively simple symmetries have been measured for their elastic moduli. Now, it is becoming necessary to measure thick composites of feasible engineering lay-ups. These generally provide the complexity of orthorhombic symmetry locally in a specimen combined with curvature in the gross structure. In this work, specimens cut from thick structures will be treated in the same way as crystals to measure the elastic moduli by means of ultrasonic wave velocities. Results on one structure will be presented. Difficulties will be analyzed.

THEORY

The generalized form of Hooke's law for an anisotropic material[1] can be written as

$$\begin{Bmatrix} \sigma_{xx} \\ \sigma_{yy} \\ \sigma_{zz} \\ \sigma_{zy} \\ \sigma_{zx} \\ \sigma_{xy} \end{Bmatrix} = \begin{bmatrix} c_{11} & c_{12} & c_{13} & c_{14} & c_{15} & c_{16} \\ c_{21} & c_{22} & c_{23} & c_{24} & c_{25} & c_{26} \\ c_{31} & c_{32} & c_{33} & c_{34} & c_{35} & c_{36} \\ c_{41} & c_{42} & c_{43} & c_{44} & c_{45} & c_{46} \\ c_{51} & c_{52} & c_{53} & c_{54} & c_{55} & c_{56} \\ c_{61} & c_{62} & c_{63} & c_{64} & c_{65} & c_{66} \end{bmatrix} \begin{Bmatrix} \epsilon_{xx} \\ \epsilon_{yy} \\ \epsilon_{zz} \\ \epsilon_{yz} \\ \epsilon_{zx} \\ \epsilon_{xy} \end{Bmatrix} \tag{1}$$

where the coefficients are the elastic constants of the material. An ultrasonic wave propagating in the solid is governed by the following equations of motion:

$$\begin{aligned} \frac{\partial \sigma_{xx}}{\partial x} + \frac{\partial \sigma_{xy}}{\partial y} + \frac{\partial \sigma_{xz}}{\partial z} &= \rho \frac{\partial^2 u}{\partial t^2} \\ \frac{\partial \sigma_{yx}}{\partial x} + \frac{\partial \sigma_{yy}}{\partial y} + \frac{\partial \sigma_{yz}}{\partial z} &= \rho \frac{\partial^2 v}{\partial t^2} \\ \frac{\partial \sigma_{zx}}{\partial x} + \frac{\partial \sigma_{zy}}{\partial y} + \frac{\partial \sigma_{zz}}{\partial z} &= \rho \frac{\partial^2 w}{\partial t^2} \end{aligned} \tag{2}$$

where u, v, and w are respectively the displacement components in z-, y-, and x-direction. The quantity ρ is the density of the material.

Review of Progress in Quantitative Nondestructive Evaluation, Vol. 9
Edited by D.O. Thompson and D.E. Chimenti
Plenum Press, New York, 1990

These equations can be specialized to the orthorhombic symmetry expected from the winding directions of -33°, +33°, and 90° relative to the cylinder axis in the thick composites, by noting that the nine elastic moduli c_{11}, c_{22}, c_{33}, c_{44}, c_{55}, c_{66}, c_{12}, c_{13}, and c_{23} will be non-zero and should have unique values. Using the coordinate system specified in Fig. 1 and the specimens cut from the composite per Fig. 2, Eqs. (1) and (2) can be solved for enough unique elastic wave velocities to permit the non-zero moduli to be computed. Equations for the moduli in terms of the velocities are given here.

$$c_{jj} = \rho v_j^2, \qquad j = 1 \text{ through } 6 \tag{3)-(8)}$$

$$c_{12} = 2\sqrt{(A_1 - \rho v_7^2)(B_1 - \rho v_7^2)} - c_{66} \tag{9}$$

where $A_1 = (c_{11} + c_{66})/2$ (10)

and $B_1 = (c_{22} + c_{66})/2$ (11)

$$c_{23} = 2\sqrt{(B_2 - \rho v_8^2)(c_2 - \rho v_8^2)} - c_{44} \tag{12}$$

where $B_2 = (c_{22} + c_{44})/2$ (13)

and $C_2 = (c_{33} + c_{44})/2$ (14)

$$c_{13} = 2\sqrt{(A_3 - \rho v_9^2)(C_3 - \rho v_9^2)} - c_{55} \tag{15}$$

where $A_3 = (c_{11} + c_{55})/2$ (16)

and $C_3 = (c_{33} + c_{55})/2$ (17)

Eqs. (3) - (8) are written for the specimens with faces parallel to the axes while Eqs. (9) - (17) are written for specimens with faces at 45° between two axes. The relevant orientations are given in Table 1 for transducer positioning and particle motion.

EXPERIMENTS

Approach

The approach is to use ultrasonic wave velocities in different directions, combined with density, to measure the elastic moduli. The approach assumes that the composite can be treated analogously to a single crystal of the same group-theoretical symmetry. This symmetry

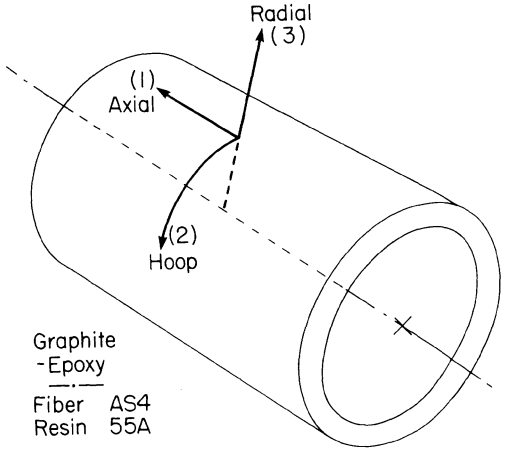

Figure 1 Material axes defined with respect to the 96 inch diameter NASA experimental rocket casing.

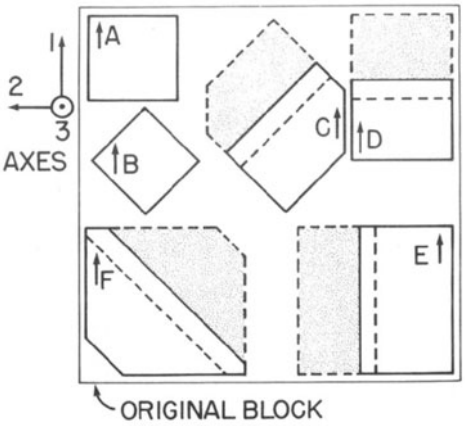

Figure 2 Ultrasonic velocity specimens cut from a slab of casing material. The stippled faces slope down at 45° from the plan view upper face.

Table 1. Set of measurements sufficient to permit calculation of the elastic moduli.

Modulus	Mode	Particle Motion Along Axis	Transducer on Plane Normal to Axis	Velocity Nomenclature	Sample	Formula Eq.
c_{11}	Longitudinal	1	1	$v_{L1} = v_1$	A	(3)
c_{22}	Longitudinal	2	2	$v_{L2} = v_2$	A	(4)
c_{33}	Longitudinal	3	3	$v_{L3} = v_3$	A	(5)
	Longitudinal	3	3	$v_{L3} = v_3$	B	(5)
c_{44}	Transverse	2	3	$v_{T23} = v_4$	A	(6)
	(Shear)	3	2	$v_{T32} = v_4$	A	(6)
c_{55}	Transverse	1	3	$v_{T13} = v_5$	A	(7)
	(Shear)	3	1	$v_{T31} = v_5$	A	(7)
c_{66}	Transverse	1	2	$v_{T12} = v_6$	A	(8)
	(Shear)	2	1	$v_{T21} = v_6$	A	(8)
c_{12}	Longitudinal	45° between 1 & 2	45° between 1 & 2	$v_{L1-2} = v_7$	B	(9)
c_{23}	Longitudinal	45° between 2 & 3	45° between 2 & 3	$v_{L2-3} = v_8$	E	(12)
c_{13}	Longitudinal	45° between 1 & 3	45° between 1 & 3	$v_{L1-3} = v_9$	D	(15)

will be determined by the winding angles of the fibers. As the parts of interest are to be cylinders, the approach also assumes that the radius of curvature of the cylinders is much larger than the wall thickness of the cylinders. This is necessary for the definition of the axes with respect to which the elastic moduli are defined. The axes must experience only infinitesimal curvature within a body of dimensions of the order of magnitude of the thickness of the cylinder wall. An analogous approach was used in pyrolytic graphite, an oriented, grown polycrystalline structure[2].

Specimens

Slabs from NASA experimental rocket case sections were procured from Hercules[3] and cut into ultrasonic specimens. Axes were defined as "1" along the rocket axis, "2" along the hoop direction, and "3" through the thickness of the casing. The fiber winding directions with respect to these axes are ± 33° from the "1" direction and at 90° to the "1" direction, i.e., along the "2" direction. The relationship of the axes to the geometry of the rocket case is given in Fig. 1. The result is orthorhombic symmetry for small specimens. Blocks as shown in Fig. 2 were cut from the large section supplied. In each block, the sides were cut such that the "3" axis at the center of the block lay along the casing thickness direction. Each block was marked (painted) with an arrow denoting the cylinder axis direction and with a letter of identification as shown in Fig. 2. Blocks A and B are rectangular parallelipipeds and permit propagation from transducers on any face. Through-transmission measurements were made for longitudinal and shear waves.

The configuration of transducers, specimens, propagation vectors $\underline{k}$, and particle motion vectors $\underline{A}$ is shown in Fig. 3. These apply generically to all specimens. In specimens C, D, E, and F, the transducers were to be placed on the face with stippled shading (shown in Fig. 2) and on the opposite parallel face. These faces are at 45° to the "3" axis and are generated by rotation about the "1" axis (for E), the "2" axis (for D), and about axes at 45° in the 1-2 plane for C and F. These cuts provide convenient specimens for ultrasonic propagation and convenient geometries for use in writing theoretical expressions linking the velocities and the moduli. One specimen with rotated faces is shown in Fig. 4 to fix ideas. Block E is shown in orthogonal projections. The locations for the transducers are given. This type of configuration allows propagation diagonally through the plies to determine the off-diagonal elements of the matrix of elastic moduli.

Ultrasonic System

The ultrasonic system is shown in Fig. 5. Through-transmission measurements were employed, as the attenuation was too high to make pulse-echo measurements. Broadband transducers of frequencies 1 MHz at 1/2-inch diameter and 1/2 MHz at 1-inch diameter were used. The pulser-receiver provided the trigger pulse to the CRO and the high-voltage pulse to the transducer; then received and amplified the transmitted ultrasonic signal for the Y-axis display. The measuring oscilloscope provided two indicators between which the delay time was

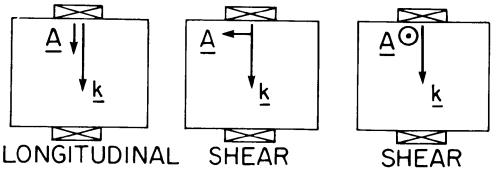

Figure 3 Drawing of the propagation direction $\underline{k}$ and the polarization direction $\underline{A}$ in a specimen for different wave modes. (Approximate for quasi-modes.)

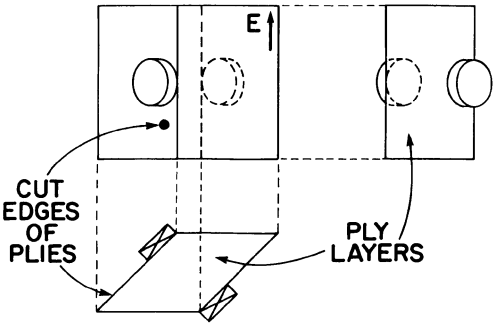

Figure 4 Diagram of one specimen cut for propagation at 45° to the ply layers.

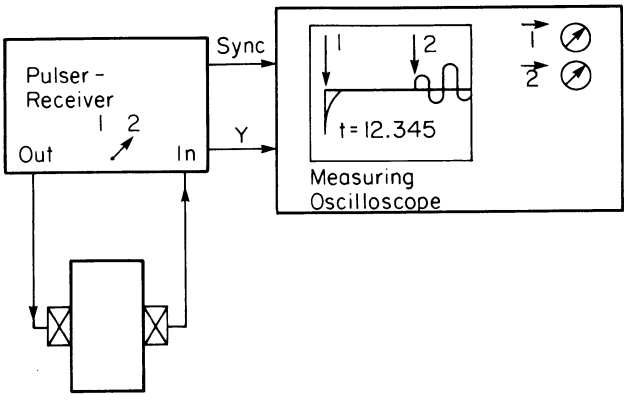

Figure 5 Ultrasonic system for measurements. Panametrics 5052 PR pulser-receiver and LeCroy 9400 digital oscilloscope.

measured. The indicators were set on the leading edges of the output pulse and the received signal.

Measurements

a. Delay in Wearplates

The delays in the wearplates of pairs of transducers were measured[4]. Hardened steel step-blocks were fabricated for this measurement. The delay in the wearplates was subtracted from the through-transmission ultrasonic time delay measurements made with the system in Fig. 5.

b. Delay, Velocity and Moduli

The ultrasonic delay between the input pulse and the leading edge of the output waveform was measured for each wave listed in Table 1 according to the method given above. This method would tend, of course, to be biased toward the frequency range within the pulse exhibiting the highest velocity if there were dispersion. Since much high-frequency energy was found to be attenuated, it is not clear what effects may be occurring. While the input was centered at 500 kHz or 1 MHz, the output waveform exhibited cycles corresponding to the range 200-240 kHz. The method used was the best available with the equipment at hand.

RESULTS

Results corresponding to the velocities named in Table 1 are given in Table 2. The delays were corrected for the wearplates and then used with the specimen thicknesses to find velocity. The velocities and the density were used to calculate the moduli. It should be noted that c_{13} and c_{23} could not be calculated, as the math resulted in complex numbers. See the second and third parts under Discussion, below.

Velocities have been measured in all the blocks, and will be reported in a later publication. It is not relevant to report others yet, as the difficulties with complex numbers are not alleviated with other modes and directions. The analysis below will show that the presence of complex numbers is a generic difficulty.

DISCUSSION

Dispersion

The results in Table 2 show some dispersion which is larger than the errors in the calculations. Moduli associated with compressional waves are slightly larger at lower frequencies, while the reverse is true for the moduli associated with shear waves. The effect is unexplained at this point in time.

Complex Numbers in c_{13} and c_{23}

Complex numbers arose in the calculation of c_{13} and c_{23} from Equations (12) and (15). These formulas contain the terms

$$13: \qquad \sqrt{(A_3/\rho - v_{L1\text{-}3}^{\ 2})(C_3/\rho - v_{L1\text{-}3}^{\ 2})} \tag{18}$$

$$23: \qquad \sqrt{(B_2/\rho - v_{L2\text{-}3}^{\ 2})(C_2/\rho - v_{L2\text{-}3}^{\ 2})} \tag{19}$$

where $A_3 = (c_{11} + c_{55})/2$

$C_3 = (c_{55} + c_{33})/2$

$B_2 = (c_{22} + c_{44})/2$

$C_2 = (c_{44} + c_{33})/2$

Table 2. Results of velocity measurements and computation of elastic moduli with $\rho = 1.4067$ g/cm^3.

Velocity			Elastic Moduli		
Nomenclature	Values (averaged if 2 equal), cm/microsec		Nomenclature	Value, 10^{11} d/cm^2	
	1.0 MHz	0.5 MHz		1.0 MHz	0.5 MHz
v_{L1}	0.69064	0.71645	c_{11}	6.7099	7.2208
v_{L2}	0.66358	0.81046	c_{22}	6.1944	9.2401
v_{L3}	0.26987	0.26694	c_{33}	1.0245	1.0024
v_{T23}	0.15552	0.15238	c_{44}	0.3402	0.3266
v_{T13}	0.15784	0.15572	c_{55}	0.3505	0.3411
v_{T12}	0.38980	0.36208	c_{66}	2.1375	1.8443
$v_{L1\text{-}2}$	0.70812	0.76727	c_{12}	3.3746	4.46164
$v_{L2\text{-}3}$	0.34849	0.40836	c_{23}	Complex	Complex
$v_{L1\text{-}3}$	0.35912	0.42035	c_{13}	Complex	Complex

With the use of the velocities v_{L1-3} and v_{L2-3} along with the previously found moduli, the parentheses in Eqs. (18) and (19) yielded positive and negative values as shown in Table 3.

A_3 itself is relatively large since it contains c_{11} which is large and would be expected to be large because it arises from longitudinal waves in the plane of the fibers. Similarly B_2 is relatively large and is expected to be, as it involves c_{22} with similar properties. At the same time, C_2 and C_3 are relatively small because they involve moduli resulting from compressing and shearing the interlaminar matrix. In order for the terms in parentheses involving C_2 and C_3 to be positive to match the terms in A_3 and B_2, the velocities v_{L1-3} and v_{L2-3} would have to be quite small. As they are moderate, not small, as can be seen from Table 2, the respective parentheses yielded negative numbers. The moduli then contained terms of the form

$$\sqrt{(+)(-)} \tag{20}$$

which are imaginary. The sums in Eqs. (12) and (15) are therefore complex.

Explanation of Excessively High Values of v_{L1-3} and v_{L2-3}

These two velocities should be low, as they involve propagation through the interlaminar material from layer to layer. It is hypothesized, however, that the values are excessively high because the wave tends to be guided along the fibers at 45° to the intended direction of propagation. See the diagram in Fig. 6. The first-arrival wave front tends to arrive at the time of earliest approach of a Huygens wavelet to the receiving transducer from a point on the transmitting transducer. The path, shown in Fig. 6 as M to N, is longer than the intended path P to N; however, M to N is traversed at a significantly faster speed as shown by the elliptical wavelet so that the time of flight from M to N is the path of least time. As this is the quantity which is measured by the present experimental equipment, the result is explicable in this fashion.

Added Effect of Attenuation

As the frequency of the pulse is lowered by selective attenuation of high frequencies, the apparent wavelength becomes longer. At the

Table 3. Signs of terms in parentheses in Equations (18) and (19).

Term Containing	Sign
A_3	(+)
C_3	(-)
B_2	(+)
C_2	(-)

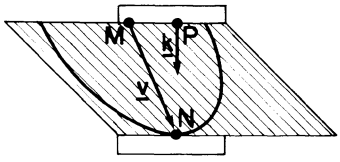

Figure 6 Diagram showing wave directions yielding excessive velocity.

received center frequency of about 200 kHz, the wavelength is comparable to the diameter of the 1/2-inch transducers, making plane wave propagation no longer relevant. The Huygens picture gains credence. The sensing of the first arrival at N from M is plausible.

Experiment to Verify Fastest Direction

In Fig. 6, the receiving transducer (bottom) was moved to the right to align even better with the fiber planes. It was found that the travel time decreased and the transmitted amplitude increased. This experiment showed that the propagation tended to be along the fiber planes.

Future Plans

To permit the measurement of c_{13} and c_{23}, an attempt will be made to construct plane wave propagation by using bursts of rf at the lower frequencies in the vicinity of 100-200 kHz which can be propagated. Some equipment which may accomplish this has become available. Also, static and/or dynamic measurements of Young's modulus, shear modulus, and Poisson's Ratio may be attempted. Theory to extract moduli from these will have to be worked out.

ACKNOWLEDGEMENTS

This work was supported by the U.S. Navy through the University of Illinois (Contract #N0014-86-K-0799) and was performed by the Center for NDE at the Ames Laboratory. Ames Laboratory is operated for the U.S. Department of Energy by Iowa State University under Contract No.W-7405-ENG-82. The findings, opinions, and recommendations expressed in this paper are those of the author and not necessarily those of the University of Illinois or the U.S. Navy.

REFERENCES

1. H. Kolsky, Stress Waves in Solids, Dover Publications, New York, 1963, pp. 33-40.

2. E. P. Papadakis and H. Bernstein, "Elastic Moduli of Pyrolytic Graphite", J. Acoust. Soc. Amer. 35, 521-524 (1963).

3. W. Murri, Hercules Aerospace Co., private communication.

4. E. P. Papadakis and B. W. Petersen, "Ultrasonic Velocity as a Predictor of Density in Sintered Powder Metal Parts", Materials Evaluation 37 (5), 76-80 (1979).